

Original Paper

## Mixing Properties of Two-Dimensional Turbulent Wall Jets and Main Flow in a Duct

Toshihiko SHAKOUCI and Sadao KUZUHARA  
(Department of Mechanical and Materials Engineering)

(Received September 2, 1982)

The mixing properties of confined wall jets and central main flow in a constant area duct are investigated experimentally. Static wall pressure, mean velocity, turbulence intensity and turbulent shear stress were measured throughout the flow field for different velocity ratios of the jet and central main flow.

### 1. Introduction

It is important to clarify the diffusion and mixing properties between jet and main flow in connection with the equipments, such as ejector, Coanda nozzle, diffuser, combustion furnace, film cooling, etc., which accompany the mixing phenomena in different flow fields.

Many studies<sup>1)~9)</sup> on the mixing phenomena concerning jet pump, ejector, etc., and on film cooling have been published. But the characteristics of the jets which spout parallel to the central main flow in the duct are not yet made clear enough.

In this paper, diffusion and mixing properties of the two-dimensional wall jets which spout into a main flow parallel to the walls of duct with constant cross-sectional area were made clear by the detailed measurements in the flow field. Under the different velocity ratios of the wall jets and central main flow, distributions of mean velocity and turbulence intensities are examined and wall shear stress to the flow direction was calculated by the Clauser's crossplot method. These results will give the useful informations to understand the transport phenomena and turbulence development of this kind of the complex flow.

## 2. Nomenclature

$B$  : width of nozzle  
(4.0 or 6.0 mm)

$C_f$  : local skin friction coefficient

$C_p$  : pressure coefficient  $\{(p - p_e) / (\frac{1}{2}\rho u_0^2)\}$

$D_i = D_0 - 2B$

$E$  : turbulent kinetic energy  
 $\{(u'^2 + v'^2 + w'^2) / u_m^2\}$

$p$  : pressure

$p_e$  : pressure at nozzle exit

$u$  : axial velocity

$u_i$  : maximum velocity of central main flow at the duct entrance ( $x = 0$ )

$u_j$  : maximum velocity of wall jet at the nozzle exit ( $x = 0$ )

$u_i', u_j'$  : the values of  $u_i$  and  $u_j$  at any  $x$  location, respectively

$u_0$  : mean velocity of wall jet at the nozzle exit

$u_m$  : mean velocity

$u_t$  : minimum velocity

$u_{0.5}$  : half velocity of  $u_j'$

$u', v', w'$  : fluctuating components of velocity in the  $x$ ,  $y$  and  $z$  directions, respectively

$-\overline{u'v'}$  : Reynolds shear stress, "-" indicates the temporal mean

$x$  : coordinate parallel to the flow direction

$y$  : coordinate perpendicular to  $x$ -axis

$z$  : coordinate perpendicular to  $x$ - $y$  plane

$\delta_m, \delta_{0.5}, \delta_t$  : distances from the side wall to the velocity  $u_j'$ ,  $u_{0.5}$  and  $u_t$ , respectively

$\varepsilon$  : eddy viscosity

$\rho$  : density

$\nu$  : kinematic viscosity

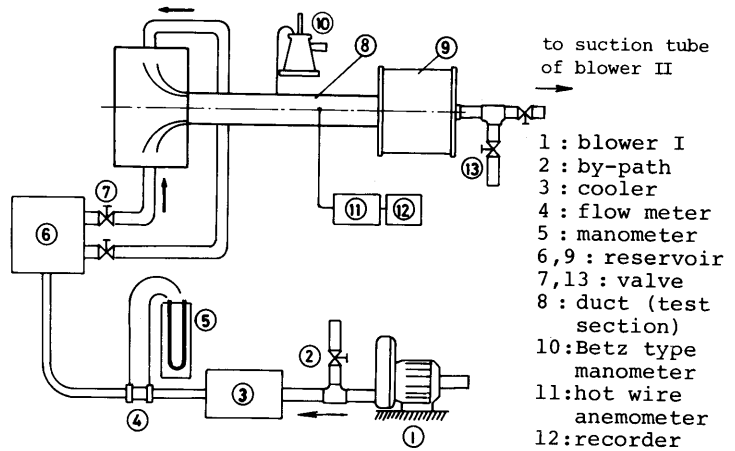


Fig.1 Schematic diagram of apparatus

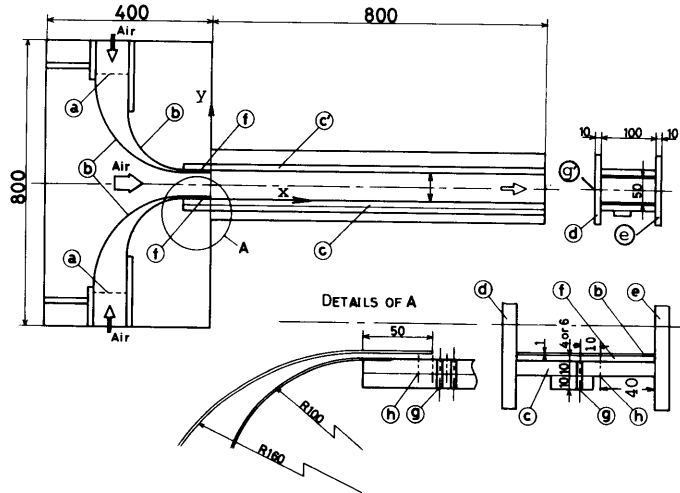


Fig.2 Details of test section

### 3. Experimental apparatus and procedure

Figures 1 and 2 show the schematic diagram of experimental apparatus and the details of the test section, respectively. Test section is symmetric with respect to the centerline of the duct. The compressed air by blower (1) is fed to reservoir (6) through cooler (3) and flow meter (5). Flow rate is controlled by by-path (2). Air from a reservoir (6) spouts, divided in two equal quantities, from bilateral nozzle (4.0 or 6.0 mm wide and 100 mm high) into a central main flow parallel to the wall of a confined duct (50 mm wide, 100 mm high and 800 mm long). The end of the duct is so followed by a blower II via reservoir (9) that any value of velocity ratio,  $u_i/u_j$ , can be obtained using flow control valve (7) and by-path (2), (13).

The side wall (c) has 20 access ports (g) for hot wire probe and 35 static pressure taps (h) which are closely located in the initial mixing region, and in the developed region in wide intervals. The upper plate (d) also has 20 access ports (g) for hot wire probe at the same interval in x direction. The plate can also be shifted in y direction, therefore measurements at any point in y coordinate are possible.

Velocity distributions,  $u$ , and longitudinal velocity fluctuation,  $u'$ , on the horizontal plane at the middle depth of duct were measured using a constant temperature hot wire anemometer held in the access ports of the side wall.

Velocity fluctuation  $v'$ ,  $w'$  and Reynolds shear stress  $-\overline{u'v'}$  were measured using a hot wire anemometer set to turn around about an axis in the access port of the side wall and upper plate<sup>10)</sup>. And eddy viscosity  $\epsilon$  was obtained by

$$\epsilon = -\overline{u'v'}/(du/dy). \quad \text{--- (1)}$$

Experiments were carried out for nozzle width  $B/D_0 = 0.08, 0.12$ , maximum velocity of wall jets  $u_j = 10$  m/sec. and velocity ratios  $u_i/u_j = 0.3 \sim 1.2$ .

### 4. Results and discussion

#### 4.1 Flow characteristics

Mix flow of the jets spouted parallel to the walls of a confined flow passage and the central main flow forms a considerable complex flow field. Such a flow is shown in Fig.4 as the general features. The flow field is divided into two different regions. The initial region, region I in the figure, consists of three different parts, namely the boundary layer between jet and side wall, the jet shear layer and central uniform velocity part. The shear layer thicken towards the downstream.

In region II, the outer edges of jets come across at the center of duct, and the velocity profile changes continuously until the flow becomes fully de-

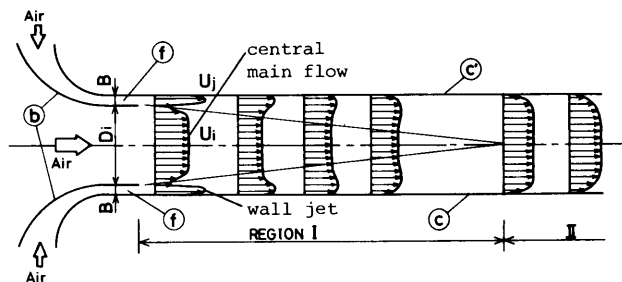


Fig.4 Flow regimes of a confined wall jets

veloped. Confined jet experiences the effect of the pressure gradient being unlike the free jet. The pressure gradient has a influence on the spread rate of jet, growth rate of boundary layer and the profile of velocity distribution. Such a flow shows a considerable complex properties.

#### 4.2 Pressure distribution on the side wall

Figure 4 is the static pressure distribution on the side wall for the nozzle width  $B/D_0 = 0.08, 0.12$  and for various velocity ratio  $u_i/u_j$ . Pressure is indicated by non-dimensional pressure coefficient  $C_p$  compared with the entrance pressure  $p_e$ . The pressures for  $u_i/u_j = 0.08$  to  $1.2$  increase rapidly in initial region, and decrease at constant negative gradient after reaching the maximum values. But their falling gradients are

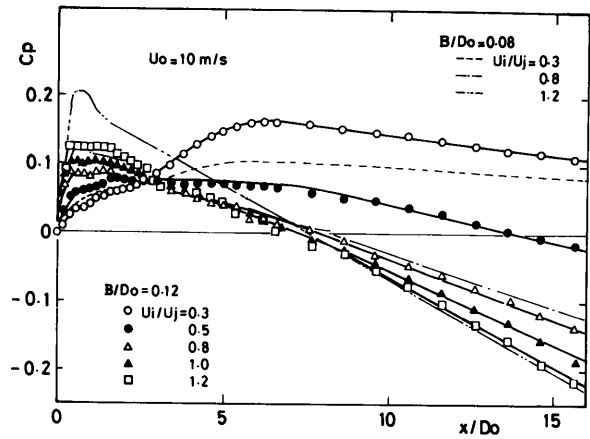


Fig.4 Static wall pressure

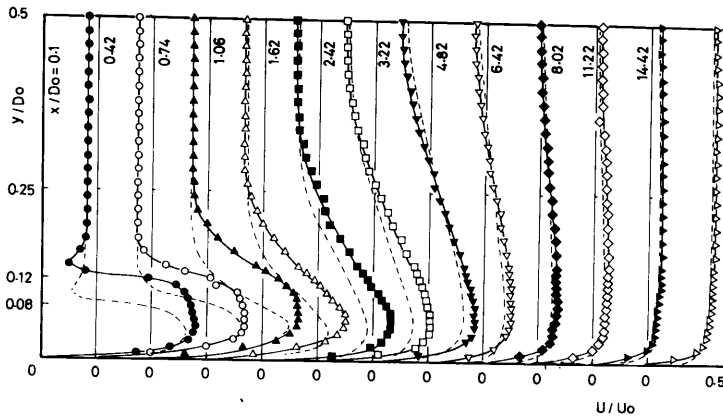


Fig.5 Velocity distribution  
( $u_i/u_j = 0.3$ )

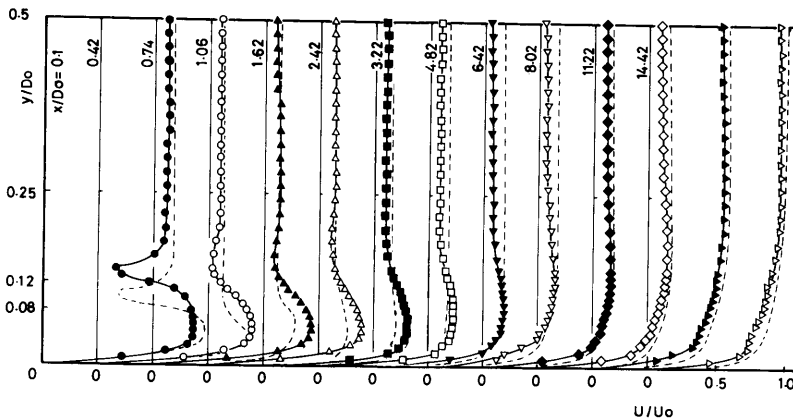


Fig.6 Velocity distribution  
( $u_i/u_j = 0.8$ )

larger than those for fully developed flow. The flow will very likely be at transition state. The gradient decreases as  $u_i/u_j$  decreases because of the decrease of pressure loss by mixing phenomenon. Maximum pressures exist between about  $x/D_0 = 0.4$  to 1.6. When the velocity ratio is smaller ( $u_i/u_j = 0.3$  and 0.5) pressures in flow direction vary as before, but the locations of maximum pressure move towards the downstream. The location where the pressure begins to decrease may exist in the boundary of the region I and II. Broken line and chain lines show the results for  $B/D_0 = 0.08$ ,  $u_i/u_j = 0.3, 0.8, 1.2$ .

In these cases, the results show the same qualitatively as shown by full lines. But the maximum pressures in region I show the larger values at the same velocity ratio.

#### 4.3 Velocity distribution

Figures 5 and 6 illustrate the mean velocity profile for velocity ratio  $u_i/u_j = 0.3$  and 0.5, respectively. Mean velocities of both of the two wall jets at the nozzle exits are held as 10 m/sec. The dotted lines in these figures are the results for nozzle width  $B/D_0 = 0.08$ . These results show only about the half width ( $y/D_0 = 0 \sim 0.5$ ) because of the symmetry of the flow field with respect to the centerline of the duct.

The features of the mixing process between the central main flow and wall jets are well understood from these figures. Shear layers exist between the wall jet and central main flow and on the side wall. The jet shear regions spread inward in the flow direction, until their inner edges reach the duct center at a position of downstream. In contrast to this, the wall boundary layer does not almost change in this region. In order to make clear the mixing properties, relations between the respective distances,  $\delta_t$ ,  $\delta_{0.5}$ ,  $\delta_m$ , from the

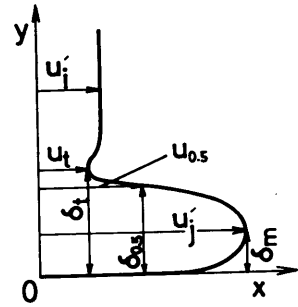


Fig. 7 Definition of reference velocity and length

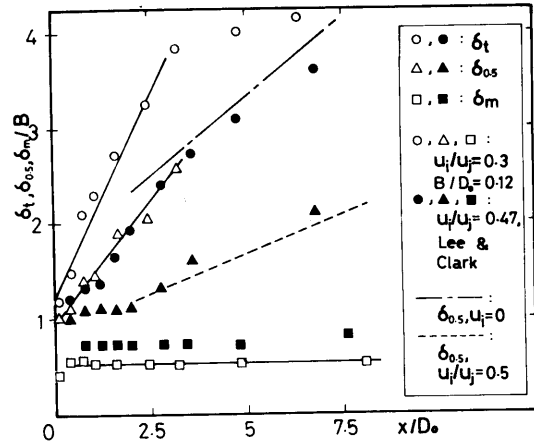


Fig. 8 Longitudinal development of mixing layers

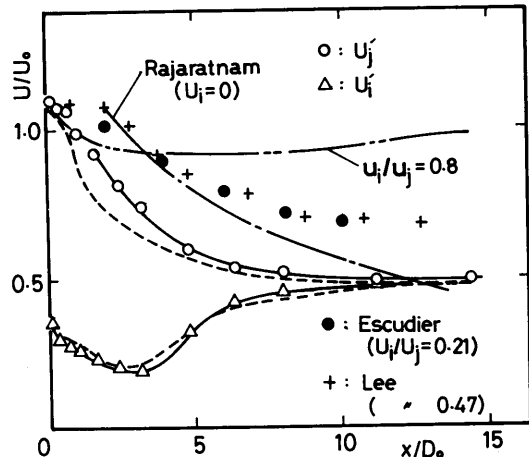


Fig. 9 Decay of maximum velocity,  $u_i$  and  $u_j$

wall to the velocity  $u_t$ ,  $u_{0.5}$  and  $u_j'$  against the distance  $x$  for  $B/D_0 = 0.12$ ,  $u_i/u_j = 0.3$  are shown in Fig.8.  $u_t$ ,  $u_{0.5}$  and  $u_j'$  denotes the minimum velocity, half velocity of  $u_j'$  and maximum velocity, respectively (see Fig.7).

$\delta_t$  and  $\delta_{0.5}$  increase rapidly towards the flow direction, but  $\delta_m$  is nearly constant in this region.  $\delta_t$  reaches the half width of the duct at about  $x/D_0 = 6.4$ . For reference, the results by Lee & Clark<sup>12)</sup>, Schwarz & Cosart<sup>13)</sup> and Rajaratnam<sup>14)</sup> are also shown in the figure. But these are the results for the case in which the confined wall causes no pressure gradient and also for different velocity ratio.

$\delta_t$ ,  $\delta_{0.5}$  for  $u_i/u_j = 0.8$  increase slowly in the flow direction because the velocity difference between  $u_i$  and  $u_j$  is small.  $\delta_m$  is also nearly constant.

Figure 9 shows the variation of maximum velocities  $u_j$  and  $u_i$  for  $u_i/u_j = 0.3$  and  $B/D_0 = 0.12$ . The dotted and chain lines in the figure indicate the results for  $B/D_0 = 0.08$ ,  $u_i/u_j = 0.3$  and  $B/D_0 = 0.12$ ,  $u_i/u_j = 0.8$ . The results for the case which has no confined wall are also shown in the figure. The maximum velocity of wall jet,  $u_j$ , decreases rapidly towards the flow direction in proportion to  $(x/D_0)^{-0.4}$ . It is known that the falling gradient is steeper than that for the case by Escudier<sup>11)</sup>, Lee<sup>12)</sup> and Rajaratnam<sup>14)</sup> in spite of the almost equal velocity ratio.  $u_j$  for  $u_i/u_j = 0.8$  decreases to the flow direction and soon reaches constant value because the velocity difference between  $u_i$  and  $u_j$  is small. After the gentle descent and rise,  $u_i$  approaches to a constant value towards the downstream.  $u_i$  and  $u_j$  for  $B/D_0 = 0.08$  experiences the similar variation in the flow direction.

#### 4.4 Wall shear stress

Wall shear stress was obtained by the crossplot method using the mean velocity profiles. Mean velocity profiles near the wall at each measuring section were plotted on the coordinates,  $u/u_i'$  and  $u_i'y/\nu$ , proposed by Clauser<sup>15)</sup> Local skin friction coefficient,  $C_f$ , was determined by the comparison of the lines of constant shear stress in Clauser chart with the above results. The lines of constant shear stress were calculated from the law of the wall

$$u/u_* = (1/k) \ln(u_*y/\nu) + c \quad (2)$$

$u_*$  : friction velocity

The value of  $k$  and  $c$  are given by Patel<sup>16)</sup> as 0.417 and 5.45, respectively. They are in good agreement in the sections of  $x/D_0 > 4.8$  for  $u_i/u_j = 0.3$  and  $x/D_0 > 1.0$  for  $u_i/u_j = 0.8$ . It is known that velocity profiles near the wall are well explained by the wall law in these sections,

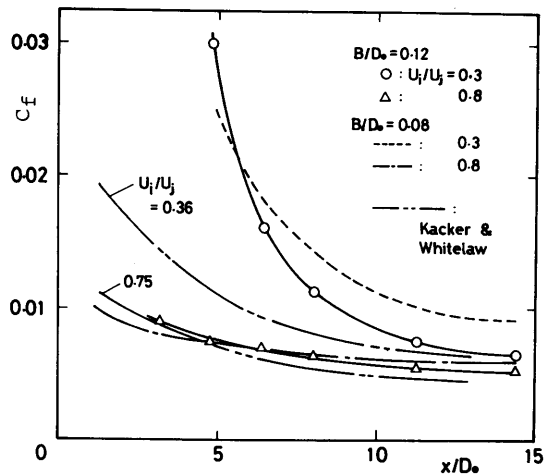


Fig.10  $C_f - x/D_0$

and the locations of agreement move downstream when  $u_i/u_j$  has a small value.

Figure 10 shows the variation of  $C_f$ .  $C_f$  for  $u_i/u_j = 0.3$  shows the large value and decreases rapidly in the flow direction, and approaches to a constant value.  $C_f$  for large velocity ratio is larger than that for the small one. It takes larger distance to reach a constant value of  $C_f$  as the velocity ratio becomes smaller. The results by Kacker & Whitelaw<sup>5)</sup> are also added in the figure. But they are the results for the case in which the confined wall has no pressure gradient and for different velocity ratio as said before. Nevertheless, their results indicate similar tendencies.

#### 4.5 Turbulence properties

##### 4.5.1 Turbulence intensities

An example of the fluctuating component distributions of velocity for  $u_i/u_j = 0.3$  is shown in Fig.11. The figure shows the distributions of the RMS value of longitudinal velocity fluctuation,  $\sqrt{u'^2}$  normalized with  $u$  for  $B/D_0 = 0.12$ . Dotted lines in the figure show the results for  $B/D_0 = 0.08$ . Two maxima of  $\sqrt{u'^2}$  value exist in the initial region of  $x$ . Their positions ( $y$ ) approximately correspond to those of  $\delta_m$  and  $\delta_{0.5}$ . One of the maxima near the wall decrease slowly to the flow direction because the turbulence generated near the wall is fed continuously into the shear layer, but another one diminishes in the downstream.

The results for  $u_i/u_j = 0.8$  also showed the similar tendencies, but the

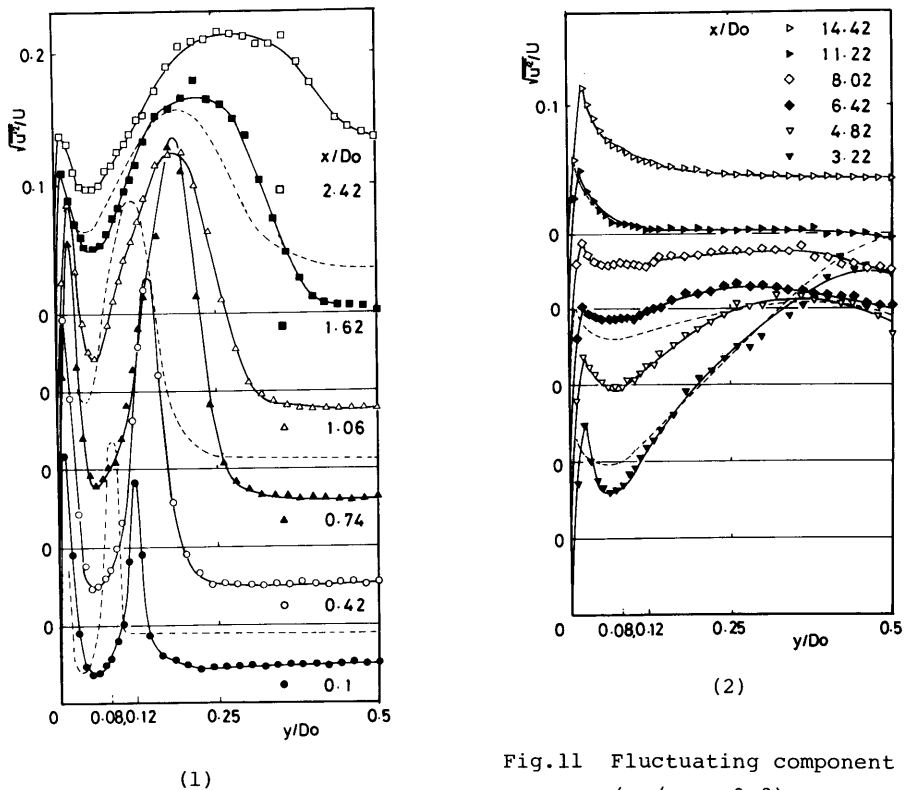


Fig.11 Fluctuating component  $u'$   
( $u_i/u_j = 0.3$ )

inner maximum was small and diminished in the downstream more rapidly than the case for  $u_i/u_j = 0.3$ . And the smaller the velocity ratio,  $u_i/u_j$ , was, the larger the value of the inner maximum became. The results for  $u_i/u_j = 0.08$  had similar properties as said above.

Figure 12 shows the velocity fluctuation  $v'$  for  $u_i/u_j = 0.3$ . The dotted lines in the figure show the results for  $B/D_0 = 0.08$ . The data close to the wall could not be obtained due to the circumstances of the measuring equipment. One maximum of  $\overline{v'^2}$  value exist in the initial region of  $x$ . Its position corresponds to the shear layer between the wall jet and the central main flow, and it diminishes towards the flow direction. The results for  $u_i/u_j = 0.08$  show the similar properties for  $u_i/u_j = 0.3$ . The velocity fluctuation  $w'$  also shows the similar properties for the results of  $v'$ .

Figure 13 shows the turbulent kinetic energy,  $E$ , for  $u_i/u_j = 0.3$ . The dotted lines in the figure show the results for  $B/D_0 = 0.08$ . One maximum exists in the profiles, and it decreases to the flow direction. Its position nearly correspond to the shear layer between the wall jet and the central main flow. The maximum value for  $B/D_0 = 0.08$  is larger than that for  $B/D_0 = 0.12$ .

#### 4.5.2 Turbulent shear stress

The distributions of turbulent shear stress for  $u_i/u_j = 0.3$  are shown in Fig.14. The dotted lines in the figure show the results for  $B/D_0 = 0.08$ .

One maximum of  $-\overline{u'v'}$  value exists in the shear layer between the wall jet and the central main flow, and it decreases in the flow direction. Its value for  $B/D_0 = 0.08$  is larger than that for  $B/D_0 = 0.12$ .

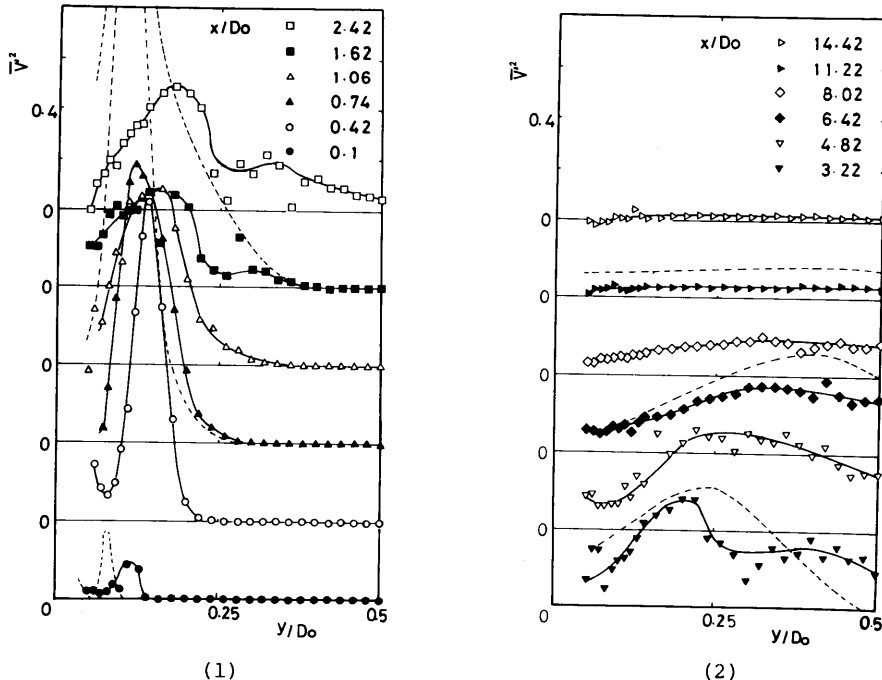
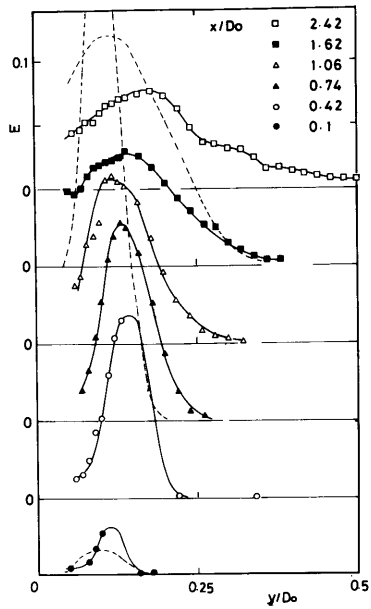
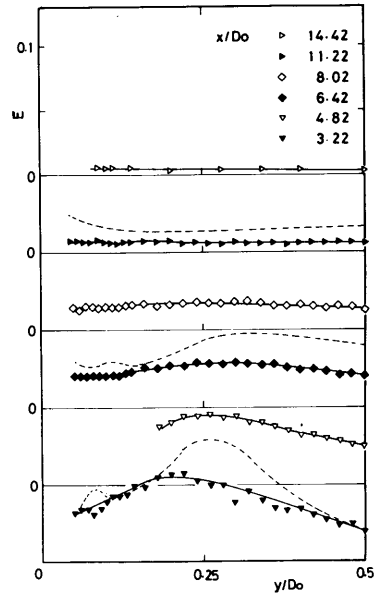


Fig.12 Fluctuating component  $v'$   
( $u_i/u_j = 0.3$ )



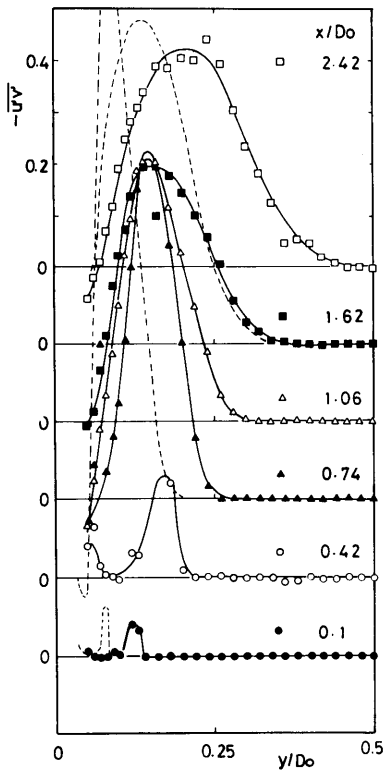


(1)

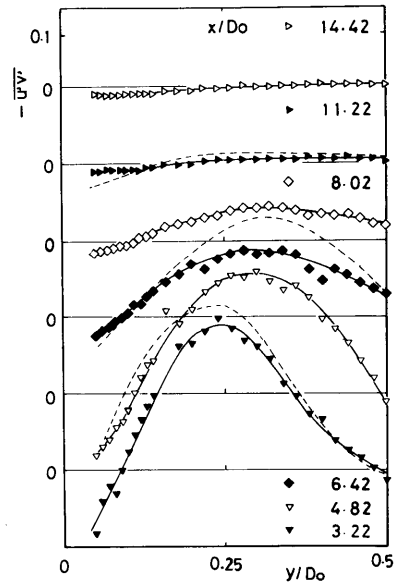


(2)

Fig.13 Turbulent kinetic energy  $E$   
( $u_i/u_j = 0.3$ )



(1)



(2)

Fig.14 Turbulent shear stress  
( $u_i/u_j = 0.3$ )

In order to understand the flow characteristics readily, namely the relations among the velocity  $u$ , fluctuating components  $u'$ ,  $v'$ ,  $w'$ , shear stress  $-\overline{u'v'}$  and turbulent kinetic energy  $E$ , their profiles for  $u_i/u_j = 0.3$ ,  $B/D_0 = 0.12$  and  $x/D_0 = 1.06$ , 11.22 are drawn in one figure (Fig.15). It is well known that each maximum value of the fluctuating component, etc., locate in the shear layer and they decrease in downstream. Same results are obtained in case of  $u_i/u_j = 0.8$ .

#### 4.5.3 Eddy viscosity

The distributions of eddy viscosity for  $B/D_0 = 0.12$  and  $u_i/u_j = 0.3$  obtained from the measurements of  $u$  and  $-\overline{u'v'}$  are plotted in Fig.16. The dotted lines in the figure show the results for  $B/D_0 = 0.08$ . It takes large value in the inner shear layer and develops to the flow direction.

#### 5. Concluding remarks

An experimental investigations on a complex confined jet mixing were conducted.

It was known that the flow patterns are divided into two types. And the development of the shear layer between the wall jets and the central main flow with the associated mixing process and turbulence development are clarified.

The distributions of the mean velocity, local skin friction, turbulent intensities, Reynolds shear stress and the eddy viscosity in the flow field which depend on the velocity ratio and  $B/D_0$  were determined.

#### Acknowledgements

The authors wish to express their gratitude to Messrs. N. Sekine, H. Tsuzuku and H. Utsumi for their cooperation.

#### References

- 1) J.T.Exley and J.A.Brighton: Journal of Basic Engineering, Trans. ASME, Series D,

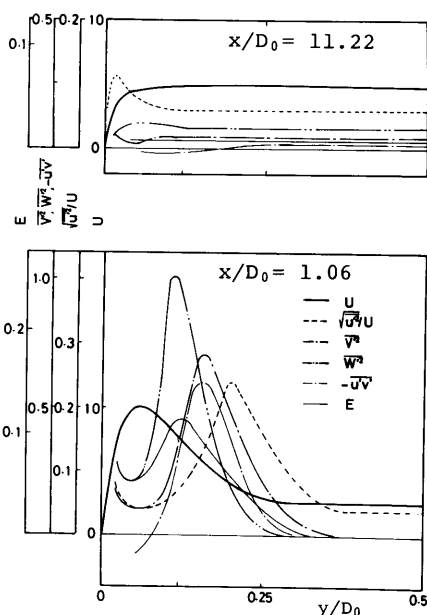


Fig.15  $u, \sqrt{u'^2}/u, \overline{v'^2}, \overline{w'^2}, -\overline{u'v'}, E$   
( $u_i/u_j = 0.3$ )

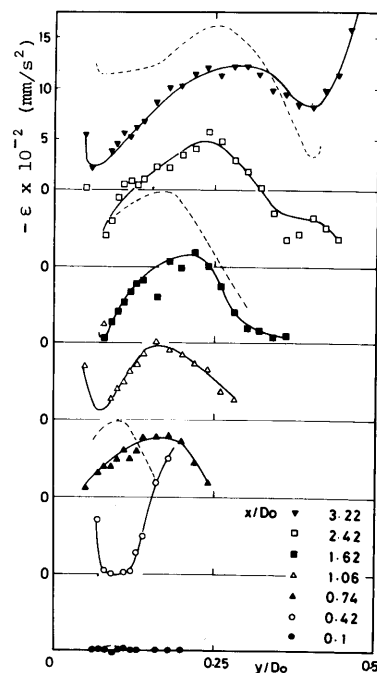


Fig.16 Eddy viscosity  $\epsilon$   
( $u_i/u_j = 0.3$ )

- 93, 192 (1971).
- 2) S.R.Ahmed: VDI-Forschungsheft, 547, 18 (1971).
  - 3) E.Razinski and J.A.Brighton: Journal of Basic Engineering, Trans. ASME, Series D, 93, 333 (1971).
  - 4) R.A.Fiedler and F.B.Gessner: Journal of Basic Engineering, Trans. ASME, Series D, 94, 666 (1972).
  - 5) S.C.Kacker and J.H.Whitelaw: Journal of Applied Mechanics, Trans. ASME, Series E, 35, 641 (1968).
  - 6) S.C.Kacker and J.H.Whitelaw: Journal of Applied Mechanics, Trans. ASME, Series E, 38, 239 (1971).
  - 7) S.Kikkawa and M.Fujii: Trans. JSME, 45-369, 1161 (1977) [in Japanese].
  - 8) L.H.Y.Lee and J.A.Clark: Journal of Fluids Engineering, Trans. ASME, 102, 211 (1980).
  - 9) M.Ljuboja and W.Rodi: Journal of Fluids Engineering, Trans. ASME, 102, 350 (1980).
  - 10) L.S.G.Kovaszny and H.Fujita: Journal of the Japan Society for Aeronautical and Space Sciences, 15-164, 289 (1967) [in Japanese].
  - 11) M.P.Escudier and W.B.Nicoll: Journal of Fluid Mechanics, 25-2, 337 (1966).
  - 12) L.Y.H.Lee and J.A.Clark: Journal of Hydraulics Division, Proc. ASCE, No. HY2, 247 (1980).
  - 13) W.H.Schwarz and W.P.Cosart: Journal of Fluid Mechanics, 10-4, 481 (1961).
  - 14) N.Rajaratnam: Journal of Hydraulic Research, 10-2, 189 (1972).
  - 15) F.H.Clauser: Journal of Aerospace Sciences, 21, 91 (1954).
  - 16) V.C.Patel: Journal of Fluid Mechanics, 23-1, 185 (1965).